An Inhibitory Neural-Network Circuit Exhibiting Noise Shaping with Subthreshold MOS Neuron Circuits

Akira Utagawa†, Tetsuya Asai, Tetsuya Hirose, and Yoshihito Amemiya

Graduate School of Information Science and Technology, Hokkaido University.
Kita 14, Nishi9, Kita-ku, Sapporo, 060-0814 Japan.
Phone:+81-11-706-7147, Fax:+81-11-706-7890
† email: utagawa@sapiens-ei.eng.hokudai.ac.jp

Abstract

We designed subthreshold analog MOS circuits implementing an inhibitory network model that performs noise-shaping pulse-density modulation with noisy neural elements. Our aim is to develop a possible ultralow-power delta-sigma-type one-bit analog-to-digital converter. Through circuit simulations we confirmed that the signal-to-noise ratio of the network was improved by 7.9 dB compared with that of the uncoupled one as a result of noise shaping.

1. Introduction

In the research reported in this paper, we aim to develop a possible ultralow-power one-bit analog-to-digital converter (ADC). A one-bit ADC converts analog input signals to digital pulse streams where the analog information is represented in the time domain. This operation is referred to as pulse-density modulation (PDM). A similar operation can be found in spiking neurons , e.g., integrate-and-fire neurons (IFNs) [1]. The firing rate of the neuron increases as the input magnitude incresases. Hence, the spike trains, e.g., the density of spikes per second, represent analog values consisting of 1-0 digital streams. Therefore a one-bit ADC could theoretically be developed by implementing such a neuron circuit on analog VLSIs. In practice, however, it is not easy to develop an ADC with a neuron circuit due to the existence of quantization, static and dynamic noises from the natural environment. The quantization noises can be eliminated by employing a sigma-delta modulator [2], but, eliminating the static noises requires an additional calibration process after chip fabrication, and eliminating dynamic noises requires a special isolation device.

In this paper, we explore a possible way to handle both static and dynamic noises in analog integrated circuits by employing neuromorphic architectures. To achieve this, we employ a population model of spiking neurons that exhibits noise shaping [3]. Through circuit simulations of the network circuit, we demonstrate that the network can improve the system's signal-to-noise ratio (SNR) as a result of effectively using the static and dynamic noises.

2. Subthreshold CMOS circuits for implementing Mar's inhibitory neural network

An inhibitory network model that exhibits noise shaping with noisy elements was proposed by Mar *et al.* [3]. This network consists of N IFNs whose membrane potential is reset to random values after each firing, whereas the synaptic weights between inputs and IFNs are randomly distributed.They demonstrated that this noisy network model could improve the SNR as a result of noise shaping as observed in conventional sigma-delta-type ADCs [2].

We implemented Mar's noisy IFN using a subthreshold CMOS neuron circuit proposed by Asai *et al.* [4]. All the MOS transistors in the circuit operate in their subthreshold region, which ensures ultralow-power consumption as a whole. Therefore, it is suitable for achieving our purpose.

Figure 1(a) shows a schematic of the neuron circuit where C_1 and C_2 represent capacitances, $V_{\mathrm{m},i}$ the membrane potential of the i-th neuron circuit, U_i the refractory potential, I_i the external input current, $I_{\mathrm{out},i}$ the quantized (spike) output current, I_{ref} the reference current for the quantization, $I_{\mathrm{d},i}$ the external fluctuation (dynamic noise), and $V_{\mathrm{I},i}$ the inhibitory input. When all the transistors are operating in their subthreshold region [5], the node equations of the circuit are given by

$$C_1 \frac{dV_{\mathrm{m},i}}{dt} = I_i - I_0 \exp(\kappa U_i / V_{\mathrm{t}}) + I_{\mathrm{d},i} \quad (1)$$

$$C_2 \frac{dU_i}{dt} = I_0 \exp(\kappa V_{\mathrm{I},i} / V_t) - I_{\mathrm{ref}} + I_{\mathrm{d},i} \quad (2)$$

where I_0 is the fabrication parameter, κ the effectiveness of the gate potential, and V_{t} a temperature dependent term. The maximum value of I_{out} is regulated by a current mirror (M3 and M4) with reference current I_{ref}.

A schematic of the network circuit is shown in Fig. 1(b). Since Mar's network model has uniform inhibitory connection strengths, we can reduce the wiring complexity from

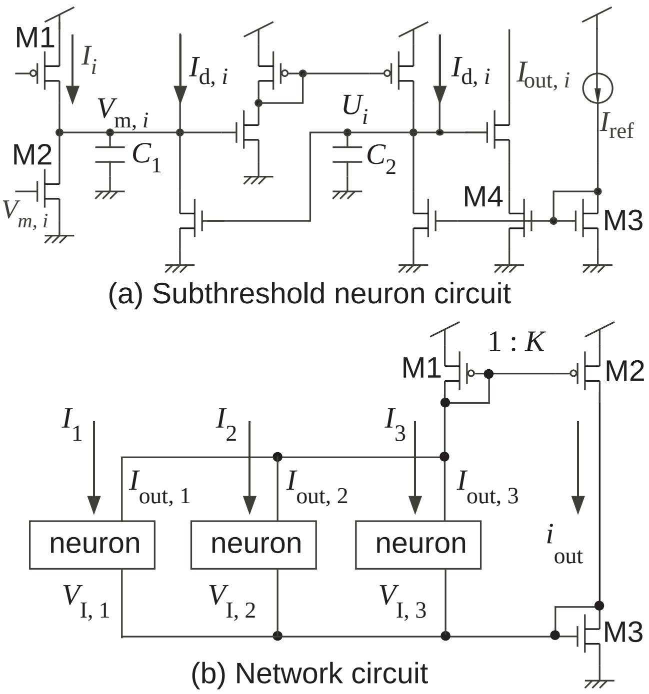

Figure 1: (a) Subthreshold neuron circuit and (b) network circuit consisting of three noisy neuron circuits and additional circuits (M1, M2 and M3) acting as a global inhibitor

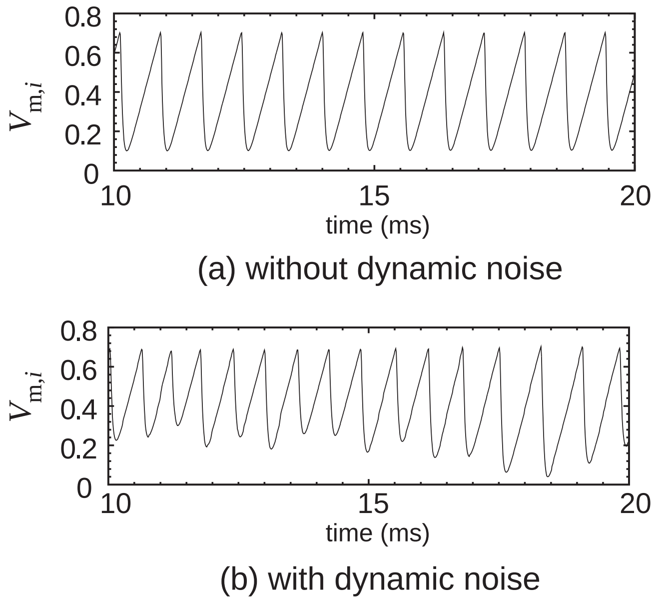

Figure 2: Time courses of $V_{\mathrm{m},i}$ for with and without dynamic noise.

$O(N^2)$ to $O(N)$ [6] by introducing a global inhibitor, which facilitates the hardware implementation. The network circuit consists of the noisy neuron circuits and additional MOS circuits (M1, M2 and M3) implementing the global inhibitor. We employ three neurons ($N = 3$) to achieve small device sizes and minimum power consumption. Current outputs of noisy neuron circuits ($I_{\mathrm{out},i}$) are summed by M1. The summed current is mirrored by a current mirror (M1 and M2) with a mirror ratio of 1:K. Therefore, the output current (i_{out}) is given by $K \sum_{i=1}^{3} I_{\mathrm{out},i}$. Since M3 in Fig. 1(b) and M2 in Fig. 1(a) forms a current mirror, membrane potentials ($V_{\mathrm{m},i}$ for all i) are decreased when i_{out} is increased, which results in the global inhibition of all the neuron circuits.

To embed the random synaptic weights (static noises) of Mar's neural network, we introduced nonuniform input current I_i for each neuron. Instead of implementing random reset of the membrane potential of Mar's neural network, we introduced dynamic noises by random current pulses ($I_{\mathrm{d},i}$), whose inter-spike-intervals (ISIs) obey the Poisson distribution, for nodes $V_{\mathrm{m},i}$ and U_i. The oscillation phase of Mar's network is increased by resetting the membrane potential, whereas that of the proposed circuit is increased by the current pulses ($I_{\mathrm{d},i}$). Therefore, applying random current pulses to nodes $V_{\mathrm{m},i}$ and U_i is qualitatively the same as the random reset in Mar's original network.

3. Simulation results

In the following circuit simulations, we assumed 1.5-μm CMOS process (MOSIS, Vendor: AMIS). First, we simulated the neuron circuit shown in Fig. 1(a) to examine the effect of the random current pulses on the circuit as dynamic noises. We assumed that MOS transistors have the same dimension of $W/L =$ 1.6μm/4μm, except for MOS transistors in current mirrors ($W/L =$ 16μm/4μm). The external analog input current (I_i) and the reference current (I_{ref}) were set to 1 nA. The capacitances (C_1 and C_2) were set to 1 pF, and the inhibitory input voltage ($V_{\mathrm{I},i}$) was set to zero. The random current pulses $I_{\mathrm{d},i}$ obeying the Poisson distribution (the mean and variation λ = 5000) were generated with an amplitude of 1 nA and the pulse width of 10 μs. Figure 2 shows the time courses of membrane potentials of noiseless ($I_{\mathrm{d},i}$ = 0) and noisy ($I_{\mathrm{d},i} \neq 0$) neurons. In Fig. 2(a), we observed periodic oscillation of $V_{\mathrm{m},i}$, whereas nonperiodic oscillation was observed in Fig. 2(b) because the phase was randomly increased by the random current pulses ($I_{\mathrm{d},i}$). Since the neuron circuit produces spike outputs ($I_{\mathrm{out},i}$) when $V_{\mathrm{m},i}$ is suddenly decreased, the operation shown in Fig. 2(b) is equivalent to randomly resetting the membrane potential after the neuron's firing.

Here, we describe how to determine the inhibitory connection strength K. Since a network with large values of K inhibits neurons severely, neurons with small inputs can not survive [3]. Therefore we have to choose an appropriate K for which all neurons can survive. Through our circuit simulations, we found that all neuron could survive when $K \leq 3$.

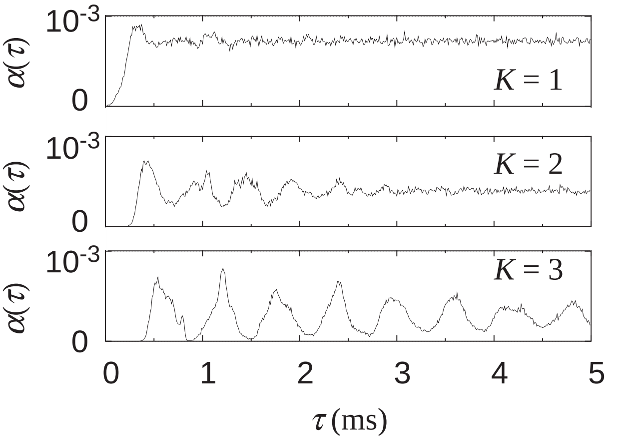

Figure 3: Auto correlation functions of output of network circuit when inhibitory connection strength K = 1, 2, and 3.

To determine the best value of K, we evaluated the performance of the PDM circuit. As described in Sect. 1, the PDM circuit produces an output spike density that depends only on the intensity of inputs in the ideal case. In other words, the PDM circuit produces spikes periodically when the inputs is constant. Therefore, we set K so that the outputs of the circuit had high periodicity. Since the auto correlation function (ACF) can quantify the periodicity of the output, it is appropriate to determine the performance of the circuit by calculating ACFs. Because the performance of Mar's model is increases in proportion to K [3], we expected that the most appropriate value of K that is 3 or less would be 3 in order to acquire the best performance. We calculated ACFs of quantized $i_{\rm out}$ [$\equiv V(t)$] where $i_{\rm out}$ was quantized to 0 (or 1) when $i_{\rm out}$ was smaller (or larger) than 0.8 nA, for K = 1, 2 and 3. Figure 3 shows the results for the ACFs with $\alpha(\tau) = \langle V(t')V(t'-\tau)\rangle$. As K increased, correlation peaks appeared and apparent periodicity was observed when K = 3. Therefore, we set K = 3 where all neurons survive and the highest periodicity is observed.

Figure 4 compares the network circuit operations when $K = 0$ (uncoupled) and $K = 3$ (coupled). When $K = 0$ [Fig. 4(a)], $i_{\rm out}$ exhibited nonperiodic oscillations. Noisy neuron circuits fired incoherently. (See raster plots in the figure. Symbols $+$, $\times$ and $*$ represent the firing events of the first, second and the third neuron circuits, respectively.) The resulting ISIs of output spike trains were random. On the other hand, when $K = 3$, $i_{\rm out}$ exhibited almost periodic oscillations [Fig. 4(b)]. The raster plots in the figure show significant differences between firing frequencies of three noisy neuron circuits as compared to the raster plots in Fig. 4(a). The resulting ISIs of output spike trains were almost uniform, as expected.

Figure 5 shows ISI histograms of the uncoupled ($K = 0$) and coupled ($K = 3$) network circuits where 1500 firing events were gathered with $\Delta = 0.01$ ms. When $K = 0$, we observed a Poisson-type distribution of ISIs (solid line in Fig. 5) because each neuron circuit was driven by independent noise sources and thus fired incoherently. When $K = 3$, a Gaussian-type distribution was observed (dashed line in Fig. 5). Once a neuron circuit receiving the maximum external input fires, the network is globally inhibited. After this firing, the neuron circuit operates in its refractory state. Therefore, ISIs of this neuron are higher than in the uncoupled case. Also, the neuron circuit cannot fire when the other neuron circuit receiving a smaller input than the maximum input, fires. Therefore, ISIs of output spike trains follow ISIs of a neuron receiving the maximum input, and the ISIs are averaged over the firing events of all neurons.

Figure 6 shows the PSD of the coupled ($K = 3$) and uncoupled ($K = 0$) networks with sinusoidal inputs ($I_i = I_0 + A\sin(2\pi f t)$, I_0 = 1 nA, A = 50 pA, f = 100 Hz) where 16 trials were averaged with a square window function. The measured SNR of the uncoupled network was 10.2 dB, while that of the coupled one was 18.1 dB, which indicated that the noise level of the coupled network was less than one tenth

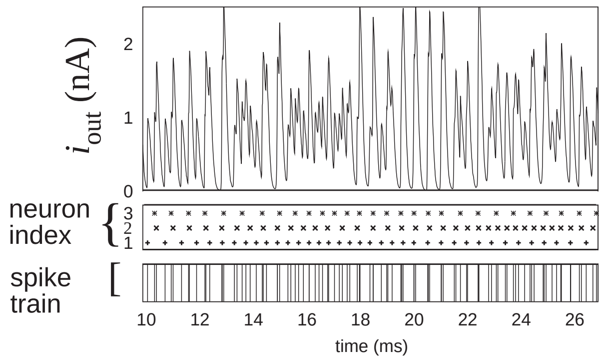

(a) uncoupled network (K = 0)

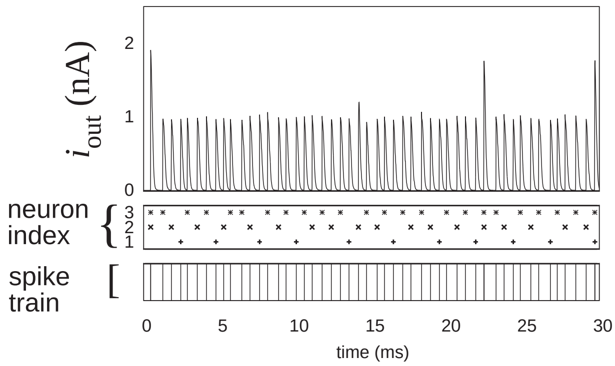

(b) coupled network (K = 3)

Figure 4: Comparison of network circuit operations when $K = 0$ (uncoupled network) and $K = 3$ (coupled network).

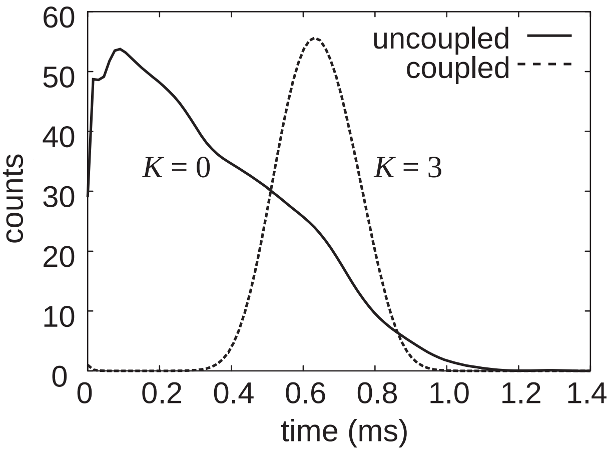

Figure 5: ISI histograms for uncoupled ($K = 0$) and coupled ($K = 3$) networks.

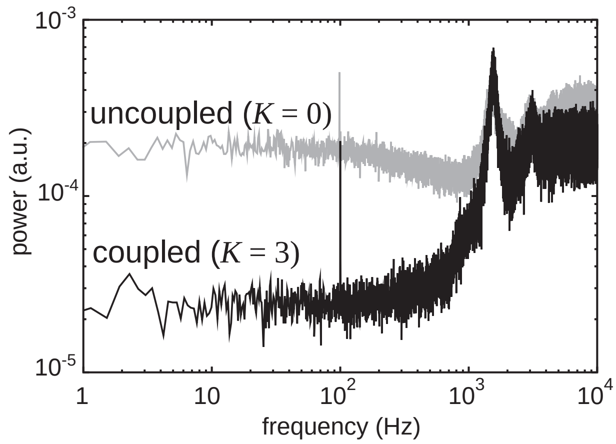

Figure 6: Power spectra of uncoupled ($K = 0$) and coupled ($K = 3$) networks.

of that of the uncoupled network below the cutoff frequency ($< 10^3$ Hz).

The external random current pulse obeying Poisson distribution is theoretically anti-correlated noise. The change in ISI distributions from the Poisson type to Gaussian type in Fig. 5 implies that the amount of noises was decreased by the effect of the global inhibition. As observed in raster plots in Fig. 4(b), individual neurons fired irregularly and thus seemed not to contribute to the signal transmission between the analog input and the digital (spike) output. Moreover, since the firing order of the neurons was also random, they seemed to fire incoherently. However, the resulting output, the sum of firing events of neurons shown at the bottom of Fig. 4(b), was almost periodic. This mechanism appeared in the resulting PSD (Fig. 6) as noise suppression, which implies that the coupled network is immune to both static and dynamic noises unlike the uncoupled network, which critically depends on the noise characteristics of individual neurons.

4. Conclusion

We investigated a possible way to develop a one-bit analog-to-digital converter in a noisy environment. We proposed a network circuit inspired by neuromorphic architectures to subtly utilize static and dynamic noises in VLSIs. We employed a population model of spiking neurons [3]. This model has a network using inhibitory coupling that exhibits noise shaping. We implemented this model with subthreshold MOS circuits to actively employ noise. The static and dynamic noise applied to the circuit for noise shaping were obtained from device mismatches of current sources and externally applied random (Poisson) spikes, respectively. A coupled network produced a Gaussian-like distribution of inter-spike intervals (ISIs), while an uncoupled one had a broad distribution of ISIs. Through circuit simulations we confirmed that the signal-to-noise ratio of a coupled network was improved by 7.9 dB compared with that of an uncoupled one as a result of noise shaping.

References

[1] M, Hovin, D. Wisland, Y. Berg, J. T. Marienborg, and T. S. Lande, "Delta-sigma modulation in single neurons," in Proc. of 2002 IEEE International Symposium on Circuits and Systems, vol. 5, 617-620, 2002.

[2] S. R. Norsworthy, R. Schreier, and G. C. Temes, ed., *Delta-Sigma Data Converters*, IEEE Press, Piscataway, NJ, 1997.

[3] D. J. Mar, C. C. Chow, W. Gerstner, R. W. Adams, and J. J. Collins, "Noise shaping in populations of coupled model neurons," *Neurobiology*, 96, pp. 10450-10455, 1999.

[4] T. Asai, Y. Kanazawa, and Y. Amemiya, "A subthreshold MOS neuron circuit based on the Volterra system," *IEEE Trans. Neural Networks*, vol. 14, no. 5, pp. 1308-1312, 2003.

[5] E .A. Vittoz, "Micropower techniques," in *Design of MOS VLSI Circuits for Telecommunications*, Y. Tsividis and P.Antognetti, Ed. Prentice-Hall, NJ:Englewood Cliffs, 1985, pp. 104-144.

[6] T. Asai, M. Ohtani, and H. Yonezu, "Analog integrated circuits for the Lotka-Volterra competitive neural networks," *IEEE Trans. Neural Networks*, vol. 10, no. 5, pp. 1222-1231, 1999.